ACTA SOCIETATIS
BOTANICORUM POLONIAE
Vol. 57, nr 1: 31-50
1988

Growth and development of shoot apex in barley. III. Study of growth rate variation by means of the growth tensor

ZYGMUNT HEJNOWICZ, JERZY NAKIELSKI, WIESŁAW WŁOCH, MAREK BEŁTOWSKI

Department of Biophysics and Cell Biology, Silesian University, Jagiellońska 28, 40-032 Katowice, Poland

(Received: June 5, 1987. Accepted: October 23, 1987)

Abstract

Silhouette of the shoot apical dome of barley does not change in time during early generative phase, although the dome height varies cyclically and increases in successive plastochrons. The elongation is limited to the dome region, the young frusta do not elongate. Relative rate of elongation (per plastochron) of the dome as a whole, decreases with increasing dome height. In the protoderm there are packets of cells distinguished by thicker walls. The growth tensor in prolate spheroidal coordinate system was applied to analysis of growth rate distribution within the dome. The meridional displacement velocities on dome surface, which are needed for the analysis, were determined on the basis of cell packet length expressed as a position function. Maximum relative elemental rate of growth occurs in subdistal zone.

Key words: *barley dome*, *growth variation*, *growth tensor*

INTRODUCTION

The shape of the barley apical dome is preserved during the vegetative phase of development, although the dome height varies (Hejnowicz and Włoch 1980a). The relative rate of growth in volume is considerably lower in the distal part of the dome than at the level of leaf primordia initiation (Hejnowicz and Włoch 1980b). Recently some aspects of natural coordinate systems (Hejnowicz 1984) and the growth tensor (Hejnowicz and Romberger 1984) have been discussed. Examples of modeling of the spatial variations of growth rates within apical domes by means of the growth tensor have also been given (Hejnowicz et al. 1984a, b, Nakielski 1987 a, b).

These efforts made possible a more rigorous description of the growth of the shoot apex of barley. For this purpose a natural coordinate system and the growth tensor have been applied to the shoot apical dome of barley. The steady shape of the dome facilitates this application. The dome has been studied during transition from vegetative to early generative phase, which is characterized by double ridge formation.

The natural coordinate system applicable to a particular organ is a system of curvilinear orthogonal coordinates in which the lines at each point of the organ are tangent to principal directions of growth (*PDG*), i.e. along them the relative elemental rate of growth in length, $RERG_l$, attains either maximal or minimal value. Cell walls alligned along principal directions of growth and initially mutually orthogonal maintain orthogonality during growth. Cell walls that are not alligned along the *PDG* but initially are mutually orthogonal, lose orthogonality during subsequent growth (Fig. 1). These properties come from the tensorial character of organ growth. Since in growing organs there is a tendency for partition walls to be inserted orthogonally to the principal directions of growth and since this orientation is preserved (see previous statement), the *PDG* can be recognized in the arrangement of cell walls.

The coordinate lines of the natural system are represented by periclines (longitudinal and latitudinal) and anticlines to which the cell walls are either

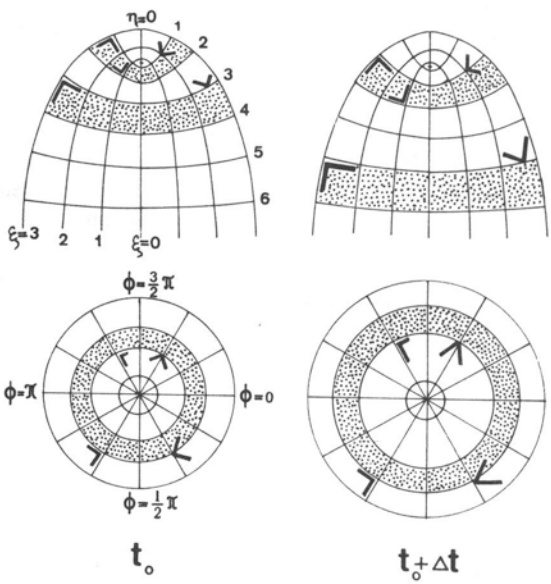

Fig. 1. An example of a natural coordinate system (η, ξ, ϕ) for an elliptical dome in longitudinal axial section (top) and in a transversal section (bottom). The pairs of orthogonal wall elements at times t_o and $(t_o + \Delta t)$ are shown. At t_o elements in the left half of the dome are along coordinate lines, those in the right are not. At $(t_0 + \Delta t)$ the elements in left halves preserve orthogonality during growth, those on the right side do not

normal or tangent. Obviously the outer periclines are then on the organ surface which means that the surface if defined by a certain value of the anticlinal coordinate.

In the case of the barley shoot apex, the arrangement of cell walls, and thus the course of periclines and anticlines, corresponds to a prolate-spheroidal coordinate system in the dome-shaped part and to cylindrical coordinate system in the bottom cylindrical part (Fig. 2). We assume that the natural coordinate system for a barley shoot apex is a prolate spheroidal system extending beyond one end of a cylindrical system. These systems are described by the following equations (Hejnowicz 1984):

prolate spheroidal system:

$$x = a \sinh\xi \sin\eta \cos\phi,$$
$$y = a \sinh\xi \sin\eta \sin\phi,$$
$$z = a \cosh\xi \cos\eta,$$

where $\xi \geqslant 0,\ 0 \leqslant \eta < \pi,\ 0 \leqslant \phi \leqslant 2\pi,$

$h_\xi = h_\eta = a\sqrt{\sinh^2\xi + \sin^2\eta},\ h_\phi = a \sinh\xi \sin\eta;$

cylindrical system:

$x = r\cos\phi,\ y = r\sin\phi,\ z = z,$

where $r \geqslant 0,\ -\infty < z < \infty,\ 0 \leqslant \phi \leqslant 2\pi,$

$h_r = h_z = 1,\ h_\phi = r.$

Application of the growth tensor needs a vector field of displacement velocities, $\bar{V}$, of material points in the apex. Such a field is described with respect to the natural coordinate system. When the shape of apex and the system of periclines are steady, as in the case of the barley apex, points are displaced along periclines. This means that the vector $\bar{V}$ has only one nonzero component, namely that corresponding to the longitudinal pericline, V_η. Thus we have:

$$\bar{V} = V_\eta(\eta, \xi)\bar{e}_\eta,\ V_\xi = 0,\ V_\phi = 0.$$

To determine the $\bar{V}$-field in the whole dome we need V_η values for points along one pericline (Hejnowicz 1984). The pericline to which there is experimental access is that on the dome surface, i.e. its meridional line. If we konw V_η on the surface which defined by $\xi = \xi_s$, i.e. we know $\tilde{V}_\eta(\eta, \xi_s)$, and the $V_\eta(\eta, \xi)$ for any point in the dome can be calculated from the equation:

$$V_\eta(\eta, \xi) = \frac{\sqrt{\sinh^2\xi + \sin^2\eta}}{\sqrt{\sinh^2\xi_s + \sin^2\eta}}\,\tilde{V}_\eta(\eta, \xi_s)$$

(the variable ϕ does not appear explicity because we assumed rotational symmetry of the dome).

At this point it should be mentioned a difficulty for $\bar{V}$ at the level $\eta = \frac{\pi}{2}$ where the two coordinate systems are "glued". At this level from the side of the spheroidal system the values of $\bar{V}$ vary with the coordinate while, when

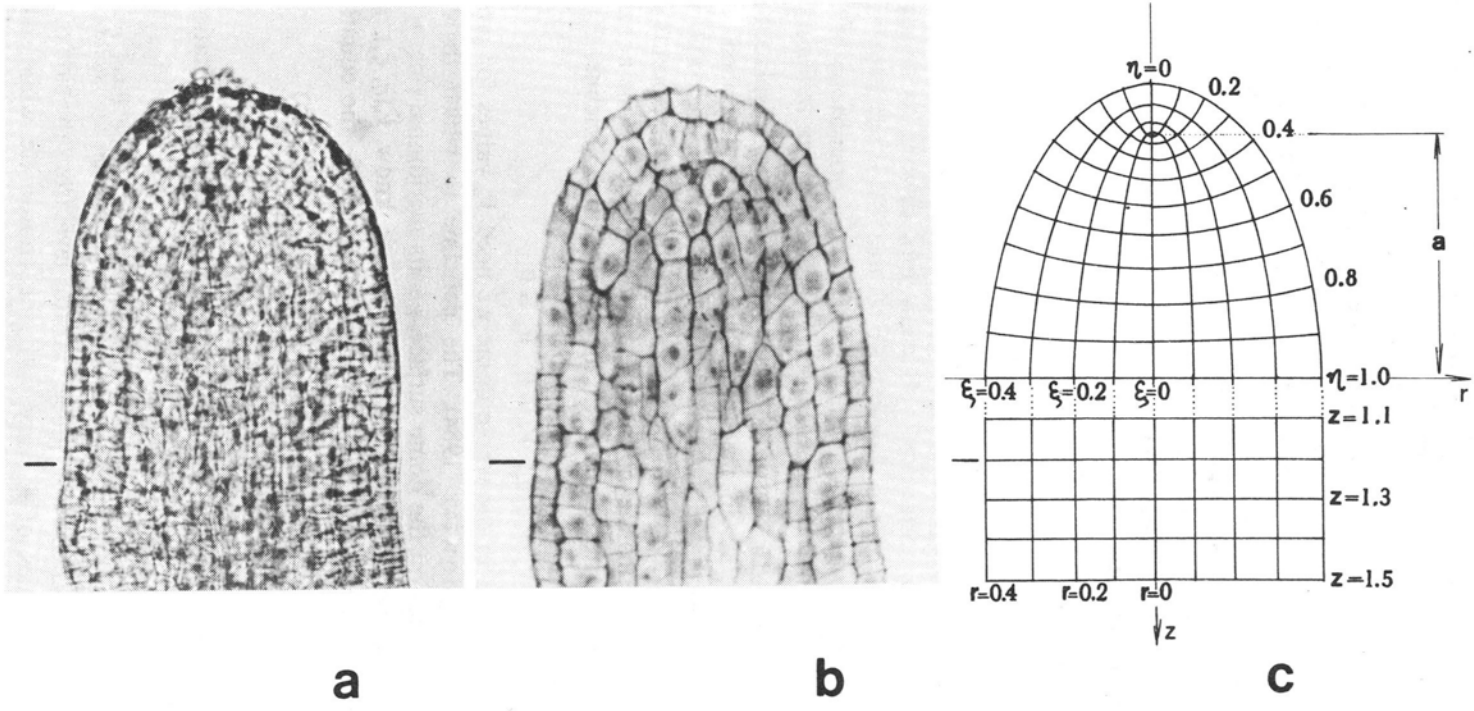

Fig. 2. Barley dome at age of 14 plastochrons: a) an intact, alive dome — optical longisection; b) axial longisection through the same dome as in (a); c) prolate spheroidal and cylindrical coordinate systems assumed as the natural. The parameter a is 84 μm, it serves also as scale marker for (a) and (b). The values of coordinates ξ and η should be multiplied by $\Pi/2$

approaching this level from the cylindrical side $\bar{V}$ does not depend on r. We are aware of this difficulty but in fact the error for the barley apex is small.

Assuming that V_η is the only nonzero component in $\bar{V}$ (which is based on empirical observations) and that $V_\eta(\eta, \xi_s)$ is known (this will be based on actual measurements), the growth tensor for the prolate spheroidal and the cylindrical systems have the following forms:

prolate spheroidal system:

$$\begin{Bmatrix} \dfrac{a^2 \sin\eta \cos\eta\,(\tilde{h}_\eta^2 - h_\eta^2)\,\tilde{V}_\eta}{\tilde{h}_\eta^2 h_\eta^2} + \dfrac{\partial V_\eta}{\partial \eta} & \dfrac{-a^2 \sinh\xi \cosh\xi\,\tilde{V}_\eta}{h_\eta^2} & 0 \\ \dfrac{\partial}{\partial \xi}\left(\dfrac{h_\eta}{\tilde{h}_\eta}\tilde{V}_\eta\right) & \dfrac{a^2 \sin\eta \cos\eta\,\tilde{V}_\eta}{h_\eta^2} & 0 \\ 0 & 0 & \operatorname{tg}\eta\,\tilde{V}_\eta \end{Bmatrix},$$

where $\tilde{h}_\eta = \sqrt{\sinh^2 \xi_s + \sin^2 \eta}$;

cylindrical system:

$$\begin{Bmatrix} \dfrac{\partial V_z}{\partial z} & 0 & 0 \\ 0 & 0 & 0 \\ 0 & 0 & 0 \end{Bmatrix},$$

where $V_z = \dfrac{dz}{dt}$.

The first tensor (for the prolate spheroidal system) has been formulated by Hejnowicz et al. (1984a), the second was discussed by Hejnowicz and Romberger (1984). Both these tensors can be formulated from the general form of the growth tensor for any coordinate system with rotational symmetry (Nakielski 1987a).

MATERIAL AND METHODS

Experimental material was of the spring barley (*Hordeum vulgare* L.) variety "Aramir". The seeds were soaked for 24 h at room temperature in well-oxygenated water changed several times during that period. They were placed on soil in trays and covered with a 5 mm soil layer. The trays were put on a window sill having a southern exposure at temp. of 16-20°C. Selection of the seedlings

and preparation for study was as described previously by Hejnowicz and Włoch (1980b). The growth rate of the individual seedlings varied, however, their morphology was the same at the same plastochronic age.

PREPARATION OF THE MATERIAL FOR PHOTOGRAPHING THE AXIAL IMAGE OF THE LIVE SHOOT APEX

The apical part of the shoot comprising the apical dome and 3-5 youngest frusta, with partially removed leaf primordia if they interfered with seeing the primordial axils, was dissected under a binocular microscope after the plastochronic age of the shoot was determined. The excised caulis was placed on a slide in a drop of water under a cover slip so that the plane of orthostichies was parallel to the slide. The axial image of the shoot apex was photographed by means of 40× objective and 10× ocular. For each plastochron, beginning with the fifth and ending with the 15th, at least 6 apices were photographed. Some apices after being photographed in vivo were individually embedded in Epon for semithin sectioning.

PREPARATION OF THE APICES TO VISUALIZE CELL PACKETS IN THE PROTODERM

A. Protoderm on the dome flank

The terminal shoot apices comprising the dome and 1-2 youngest leaf primordia were dissected at different plastochronic ages of the seedlings and processed individually. The apex was first photographed in vivo and then fixed in 3% glutaraldehyde pH 7 for 8 hours at room temperature and stored until the next day at 0°C. Thereafter it was washed, first in distilled water, and then in tap water for 1 h, transferred to periodic acid for 1 h at 0°C and then to leucofuchsine for 1 h (PAS method). After washing, apices were dehydrated in an acetone series and embedded in Euparal between two cover glasses in a position such that the plane of orthostichies was parallel to the glasses. The preparations after drying were mounted on microscope slides and microphotographs were made using 63× objective and 10× ocular, during which the microscope was focused on the upper protoderm on the flank of the apex. The preparation was then turned over and the protoderm on the other side was photographed. Each apex thus provided a pair of photographs showing opposite flanks of the protoderm. Examples of protoderm images are shown in Fig. 7.

B. Protoderm on the summit

The dome was dissected from the leaves and excised at a level of about 80 μm beneath the vertex and then was treated as described in A. The stained

and dehydrated dome was embedded in Euparal on a glass slide under a cover slip in such a position that its base was in contact with the slide. Photomicrographs were made of the protoderm at the tip, Fig. 6.

RESULTS

GENERAL CHARACTERISTICS OF GROWTH DISTRIBUTION BASED ON STUDY OF LIVE APICES

Figure 3 shows the positions of the vertex and leaf axils in the caulis ordered according to plastochronic age of the apex. The position of the axil of the *n*-th leaf was interpolated by a smooth line drawn by hand. These lines are nearly straight and parallel, which indicates that the elongation of the caulis is mostly localized within the dome. Figure 4 shows the position of the vertex as it changes with plastochronic age, when the position of leaf no 7 (interpolated in Fig. 3) is put on the same horizontal level. When this is done it is evident

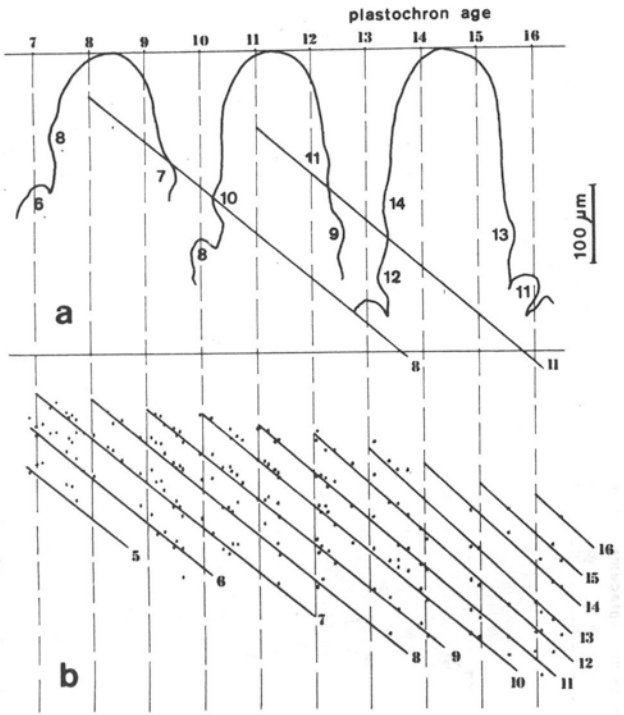

Fig. 3. Diagram of caulis elongation in *Hordeum* plotted on the basis of analysis of the plastochron age and dimensions of apices photographed in toto and in vivo: a) arrangement of three apices illustrating the construction of the diagram; the apex axis intersects the time coordinate at points corresponding to dome age; b) plots of caulis growth as the function of plastochron age, the points on perpendicular axis corresponding to levels of axils of a particular leaf, numbered sequentially from the shoot base, are joined by lines. The lines were interpolated by hand on the basis of data from 71 apices (dots)

that the axils of the leaves of the 8th and successively higher plastochrons are on the same horizontal levels in shoots of increasing age. This means that the frusta in the apical portion of the caulis do not grow in length. The elongation is limited to the apical dome. The major part of the new volume produced by its elongation growth is exported from the dome in the newly-formed frusta,

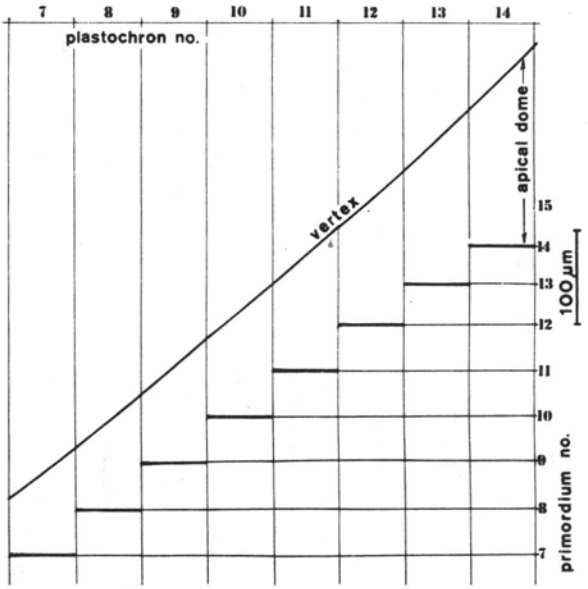

Fig. 4. Position of the vertex when the position of the axil of leaf is not parallel to the time axis, as it was in Fig. 3b. The position of axils of other leaves are on horizontal lines which indicates zero elongation for young frusta

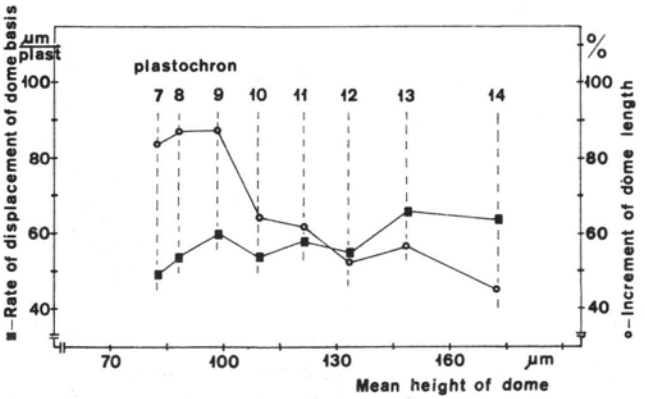

Fig. 5. Mean rate of displacement of dome base during successive plastochrons, indicated above points, and mean increment of dome length in % of length at the beginning plastochron, plotted against the mean height of the dome (evaluations based on position of axil of uppermost primordium with respect to the vertex)

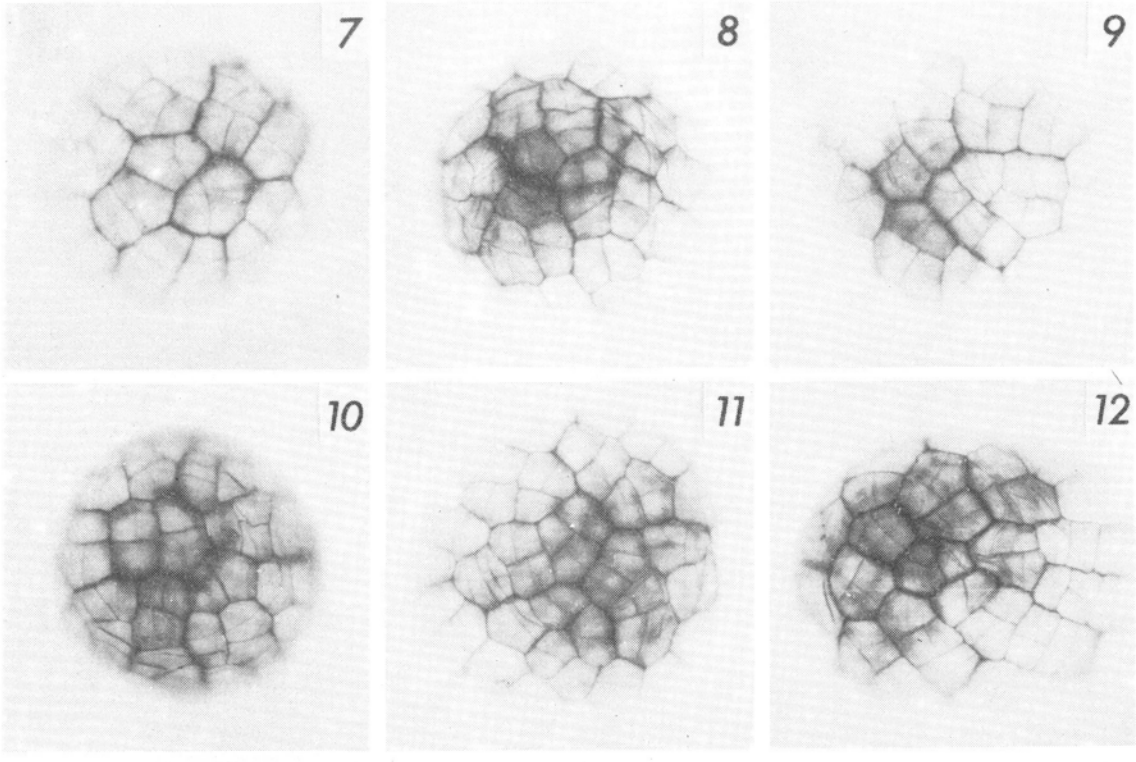

Fig. 6. The protoderm on dome summit for the shoot apex at different ages. The plastochron age of the dome is indicated in right upper corner. The position of the vertex is not necessarily at the center of each photograph

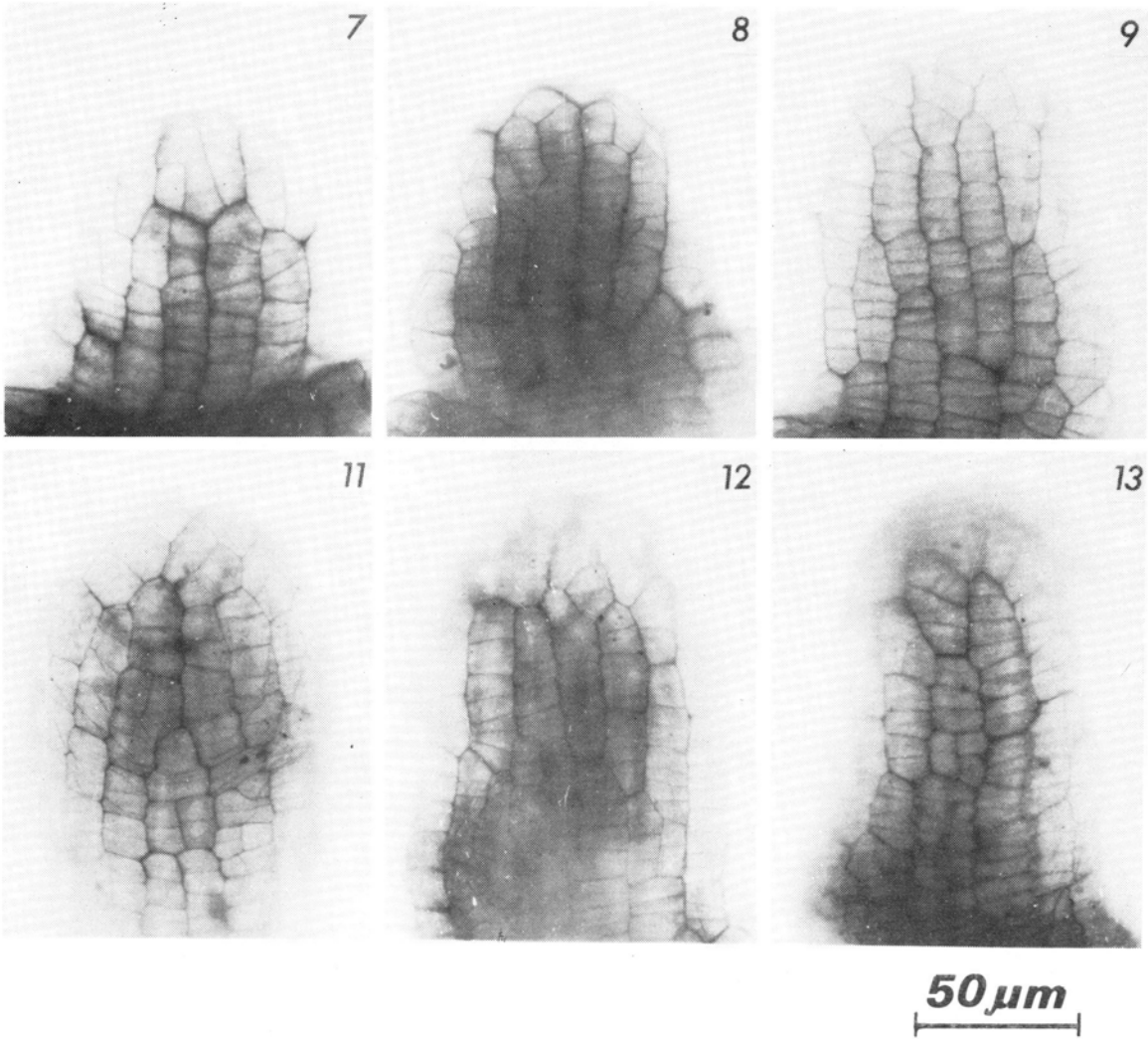

Fig. 7. The protoderm on dome sides. The plastochron age appears in the upper right corner

but a minor part of it is "invested" into the dome itself, and its height increases with age. The apical dome elongates by 49 μm during the 7th plastochron (which begins with the initiation of the leaf no. 7) and by 64 μm during the 14th plastochron. The rate of displacement of the vertex is 49 μm per plastochron during the 7th plastochron when the mean distance of the base from the vertex is 82 μm, and the rate is 58 μm/plast. during the 11th plastochron when the distance is 122 μm. Thus the rate of displacement increased only by 18% while the mean height of the dome increased by 49%. During the 14th plastochron the mean height of the dome was 173 μm while the displacement rate was 64 μm/plast. In comparison to 11th plastochron the rate increased by only 10% while the height increased by 42%. This means that the rate at which the dome base is displaced from the vertex changes considerably less than the dome height (Fig. 5). The relative rate of elongation of the apical dome decreases sharply in 10th plastochron and this trend is maintained further with increasing dome height (Fig. 5). The height exported as the dome passes from the end of the 7th to beginning of the 8th plastochron is 45 μm and 41 μm during the 14/15 plastochron. Relative rate of elongation of the apical dome decreases during successive plastochrons; during the 7th plastochron the elongation was 84% of the initial length, during the 14th plastochron it was 45%. The simplest explanation of the decrease of relative rate of elongation of the whole dome with increasing dome height is that its basal part elongates much less than the mean relative rate of the remaining part of the dome. Taking into account the results of our previous study that the distal part of the dome grows slower than the proximal part, we can expect a maximum rate of growth somewhere within the dome. What is the distribution of growth rates within the apical dome? This question will be answered by means of the growth tensor.

CELL PACKETS IN THE PROTODERM

In the protoderm there are packets of cells distinguished by thicker walls (Figs. 6, 7). A packet is a group of cells enclosed within a wall that at one time was the wall of a single cell. From this cell all the cells in the packet originated by successive divisions. At the summit there is usually either a packet which includes the vertex (Fig. 6 (pl. 10)), or a group of 2 or 3 packets which are in contact at the vertex (Fig. 6 (pl. 11)). Orientation of the packet walls (p-walls) is different but two main groups are: meridional (longitudinal) and latitudinal (transverse). Moving along a meridian from the vertex one crosses the first transverse p-wall then the next one. The meridional distance between the two first p-walls embraces mostly two cells. It appears that a cell slightly removed from the vertex becomes a mother cell for a packet. As the dome grows, this packet is displaced and simultaneously its length increases. Figure 8 shows packet length l_m plotted against meridional distance m for apices at 8th and

14th plastochron. The points become increasingly dispersed with increasing meridional distance. We interpret this as a consequence of different initial packet lengths. Similar plots were made for apices of other plastochronic ages. All were similar in the distribution of the points. The plots were interpolated by means of a least squares method for determining 2nd order polynomial regression. The interpolating lines were quite similar for apices at different ages. Therefore for further study we used the line for the 8th plastochron.

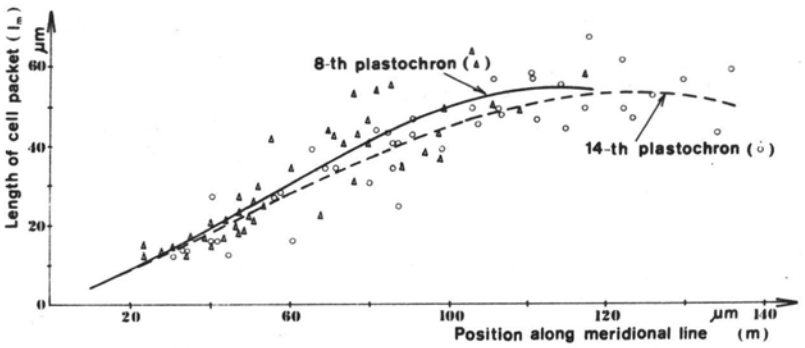

Fig. 8. Plot of cell packet length versus meridional distance of its center from the vertex for apices in 8th and 14th plastochrons

According to our hypothesis, when the apical end of one packet is displaced to the position which was initially occupied by the basal end of this packet, the apical end of the next packet is displaced to the initial position of its basal end and so on, i.e. that the walls separating packets are displaced along the length of the packets in the same time interval Δt (Fig. 9). Displacement along a packet length means that l_m can be considered as an increment of distance m of the wall during the interval Δt, thus the line describing l_m as a function of m can be interpreted as the line of displacement velocity $\frac{\Delta m}{\Delta t}$ being a function of m. This rate can be scaled in units of μm per plastochron, because we know the rate at which the base of the dome moves. The packet length at the dome base at $m = 120$ μm is 54 μm. This can be read in terms of $\frac{\Delta m}{\Delta t}$ as $\frac{54\ \mu m}{\Delta t}$ (where Δt is the time interval for shifting the packet pattern for one packet length) which corresponds to velocity 53 μm per plastochron of the displacement of dome basis from the vertex. Thus $\frac{54\ \mu m}{\Delta t} = 53$ μm/plast. which indicates that Δt is about 1 plastochron, which in itself is an interesting result.

$\frac{\Delta m}{\Delta t}$ is a displacement rate estimated for a relatively long time increment and in relatively long segments. We need a similar displacement rate but one that

can be more accurately described $\frac{dm}{dt}$. No doubt there is a strict relationship between $\frac{\Delta m}{\Delta t}$ and $\frac{dm}{dt}$, but would that be justified using the function $\frac{\Delta m}{\Delta t}(m)$ as representing the function $\frac{dm}{dt}(m)$? Not knowing whether we could to this, we used a more rigorous procedure involving the function $l_m = f(m)$.

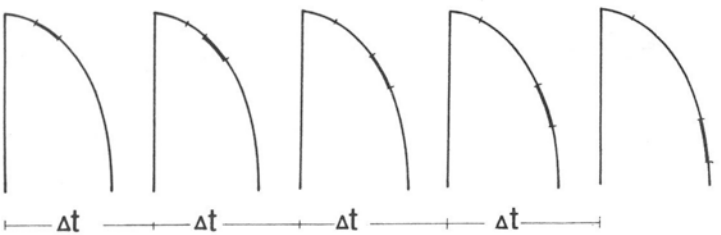

Fig. 9. Representation of the idealized dome (right half only) at intervals Δt apart. The position of the cell packets is based on the assumption that the pattern of packet length is steady; Δt is the interval necessary to displace a packet to the position initially occupied by next packet. One packet is marked

Assuming that the interpolating line in Fig. 8 correctly describes the change of packet length as it is displaced during growth we can reconstruct on the basis of this line the idealized sequences of packet lengths along a meridian. We start with the packet l_1 the center of which is located at m_1. The apical end of this packet is at $m_1 - \frac{1}{2}l_1 = m_1 - \frac{1}{2}f(m_1)$, the basal end is at $m_1 + \frac{1}{2}f(m_1)$. The center of next packet is at $m_2 = m_1 + \frac{1}{2}f(m_1) + \frac{1}{2}f(m_2)$ because the apical end of this packet coincides with the basal end of the previous packet, thus $m_1 + \frac{1}{2}f(m_1) = m_2 - \frac{1}{2}f(m_2)$. We can find m_2 if we know m_1 and two functions of m: $A = m - \frac{1}{2}f(m)$ and $B = m + \frac{1}{2}f(m)$, these functions are represented graphically in Fig. 10. The functions A and B show also a way of evaluating m_2, m_3, m_4, namely, if m_1 is known the center of next packet (m_2) can be found, and so on.

Figure 11 shows the construction pertaining to the relation between the position along m and time for barley apex. More points for the plot m versus t can be obtained by using sequences for packet length, having different location of the first packet. In this way we can approximate the functional dependence between m and t, $m = m(t)$ as closely as we like. From the resulting plot of this function we can read the number of plastochrons needed to displace a cell from

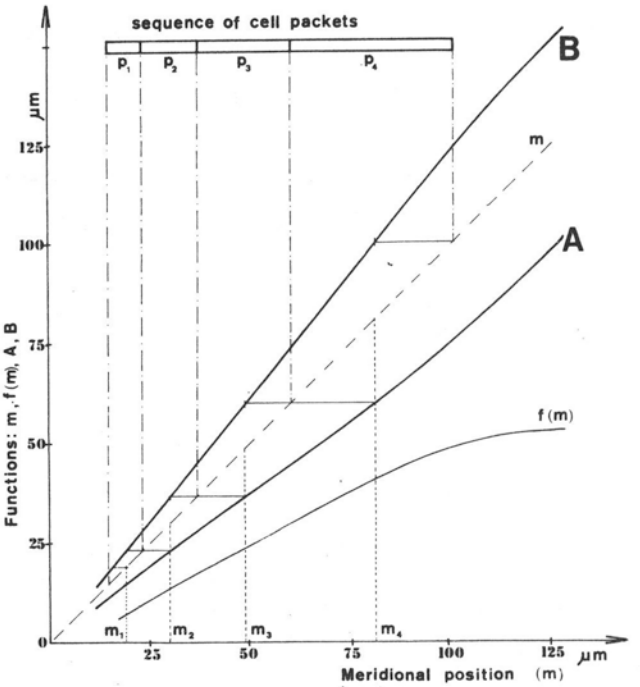

Fig. 10. Diagram showing the functions $A = m - \frac{1}{2}f(m)$ and $B = m + \frac{1}{2}f(m)$ and the method of obtaining the sequence of cell packets if the center of first packet is located at m_1 (see text). Function $f(m)$ is the same as l_m plotted against m for the apex in 8th plastochrons in Fig. 8

a certain position in the distal part of the apex to its base. If, for instance, we consider a cell the basal end of which is on the anticline 20 μm (Fig. 12), the basal end of the clone deriving from this cell will appear after 5 plastochrons at the anticline 105 μm, which is at the level of leaf initiation. This means that in the dome which is, for instance, 12 plastochron old, the dome base subtends the clone which derived from the cell subtended by the anticline at 20 μm during the 7th plastochron. If the considered cell has initially periclinal dimension 8 μm the length of the clone derived from it after 5 plastochrons is 60 μm in this direction.

From the function $m = m(t)$ the derivative $\frac{dm}{dt}$ which is equivalent to $V_m(t)$ on dome surface, can be obtained, and can be plotted as a function of m (Fig. 13). We have to express $V_m(m)$ as a function of the curvilinear coordinate η. This can be achieved by means of the relation between m and η. We used $V_m(\eta)$ data obtained in this way in tensor analysis. We also need the derivative $\frac{dV_m}{d\eta}(\eta)$. The derivative was obtained graphically (Fig. 14). Both functions $V_m(\eta)$

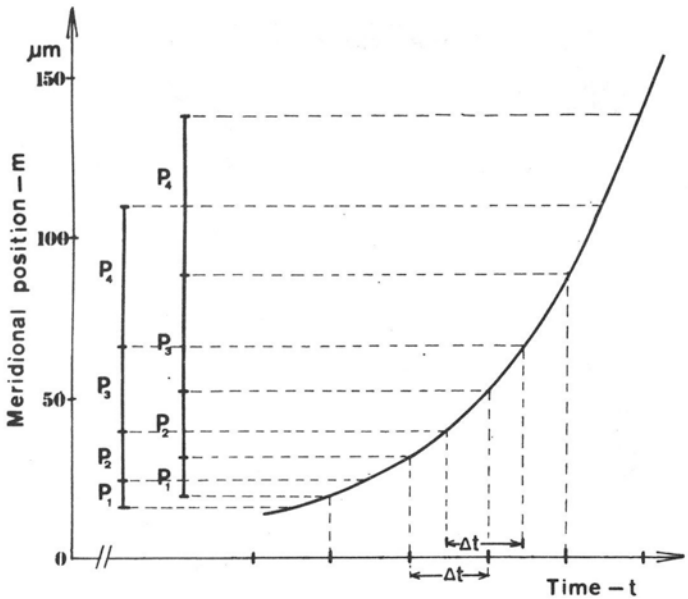

Fig. 11. The relationship between position and time for sequences of cell packets. During the time interval Δt (one plastochron) the apical end of a cell packet is displaced for the length of this packet. The detailed line $m = m(t)$ was obtained by superposition of points (position versus time) for several sequences of cell packets with different position of the first packet. Two cell sequences are indicated

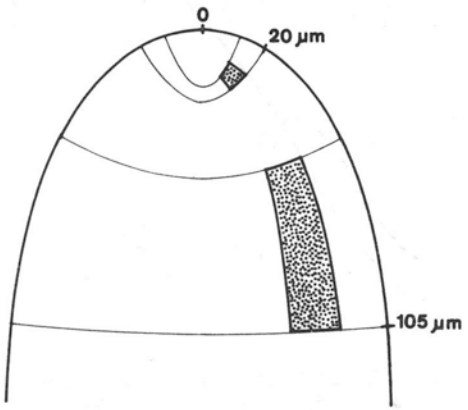

Fig. 12. Diagram showing a cell delineated from below by the anticline which crosses the dome surface 20 μm from the vertex at $t = 0$, and the length of the deriving clone when its lower boundary reaches the anticline at 105 μm. The latter length is attained after 5 plastochrons, $t = 5$

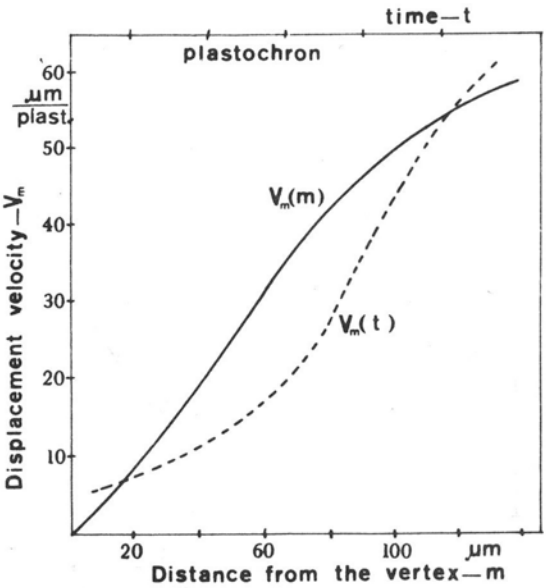

Fig. 13. Displacement velocity V_m on dome surface as the function of position (full line) and as the function of time (broken line). The latter was derived by differentiation of the function $m(t)$ in Fig. 11. $V_m(t)$ was transformed into function $V_m(m)$ on the basis of the relation between position and time shown on Fig. 11

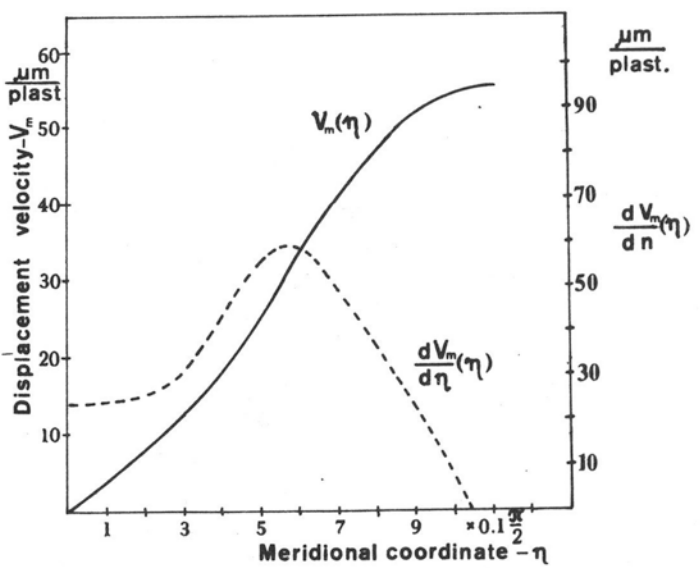

Fig. 14. Displacement velocity V_m as the function of periclinal coordinate (full line) and its derivative with respect to η (broken line)

and $\frac{dV_m}{d\eta}(\eta)$ were read from the graphs and digitized for using them in a computer for calculating *RERG* values.

DISTRIBUTION OF GROWTH RATES

As mentioned in introduction $V_\eta(\eta, \xi)$ and its derivative for any point in the dome can be calculated if $V_\eta(\eta, \xi_s)$ is known along a pericline on dome surface. Namely

$$V_\eta(\eta, \xi) = \frac{\sqrt{\sinh^2 \xi + \sin^2 \eta}}{\sqrt{\sinh^2 \xi_s + \sin^2 \eta}} \tilde{V}_\eta(\eta, \xi_s)$$

and $$\frac{\partial}{\partial \eta} V_\eta(\eta, \xi) = \frac{\sqrt{\sinh^2 \xi + \sin^2 \eta}}{\sqrt{\sinh^2 \xi_s + \sin^2 \eta}} \frac{\partial \tilde{V}_\eta}{\partial \eta} + \tilde{V}_\eta \cdot \frac{\partial}{\partial \eta} \left(\frac{\sqrt{\sinh^2 \xi + \sin^2 \eta}}{\sqrt{\sinh^2 \xi_s + \sin^2 \eta}} \right).$$

Figure 15 shows the $RERG_l$ (relative elemental rate of growth along a line) in different directions at different points. In Fig. 15a the anticlinal *RERG* is that

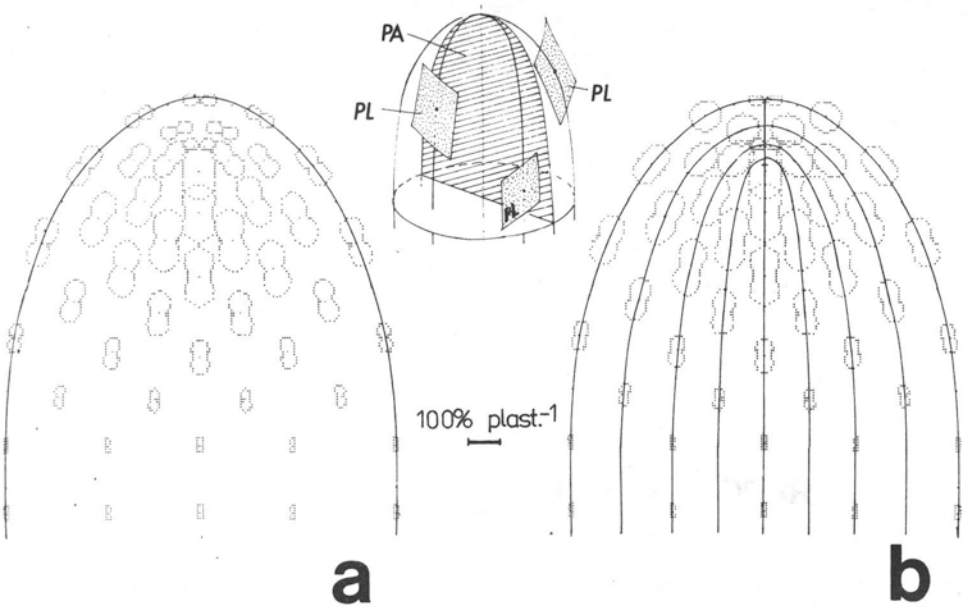

Fig. 15. Variations of relative elemental growth rates in length within apical dome in the axial plane PA (a) and in the plane PL (b) tangent to longitudinal and latitudinal periclines at a point. Three dimensional drawing in the center shows the orientation of some planes PA and PL in the dome. Values of the $RERG_l$ are displayed in the form of two dimensional computer generated plots of $RERG_l$ around a number of points lying in the axial plane at nodes of coordinate net (for the plots in b the latitudinal direction is oriented anticlinally as the result of the rotation of each PL plane by 90° around pericline). Plots of $RERG_l$ are drawn in the same scale

indicated by the narrowing of the indicatrice plot, i.e. it represents the minimal principal growth rate. The periclinal $RERG_l$ is the maximal principal growth rate. Figure 15b shows the indicatrice cut by the plane tangential to the point so that periclinal $RERG_l$ and latitudinal $RERG_l$ are seen. The $RERG_l$ latitudinal at each point is smaller than $RERG_l$ periclinal and larger than $RERG_l$ anticlinal (it is the mixed principal growth rate). It may be seen that the principal growth rates are higher in the inner portion of the distal part of the dome. There is small decrease of the rates close to the tip and very pronounced decrease in the proximal (basal) part of the dome.

Figure 16 shows the pattern $RERG_{vol}$. The pattern is characterized by increases in the rate with distance from the tip up to a maximum at about 30-35 μm along the meridian which is the level slightly above the leaf initiated in the 9th plastochron but is quite high above the emergence of the double ridge in the 14th plastochron. The data of Fig. 15 and 16 provide answer to the main question: what is the distribution of growth rates within the dome.

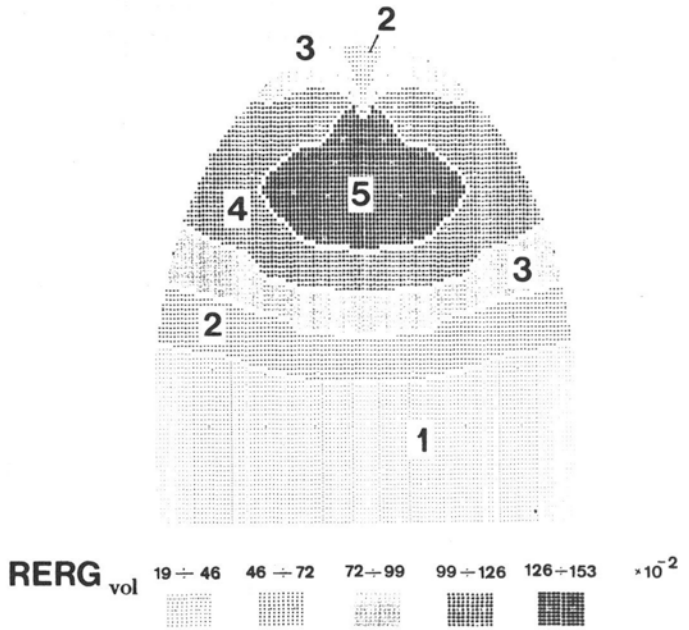

Fig. 16. Variations of volumetric relative elemental growth rate ($RERG_{vol}$) in the apical dome. The full range of $RERG_{vol}$ after interpolation was divided into 5 equal parts, numbered from 1 to 5. The program SYMAP was used to get the regions on the map

DISCUSSION

The shape of apical dome is usually taken as its geometrical form irrespective of scale. E.g. Abbe and Phinney (1951) wrote that the dome of

maize was constant in shape (half of an ellipse on medial sagittal section), although the height and thickness of ellipsoidal dome increased proportionally during successive plastochrons. Similarly, Rogan and Smith (1974) wrote in their study of shoot apex of *Agropyron*: "the height and diameter change in proportion to maintain a continuous shape". In the present paper the steadiness of shape of barley dome is taken as constant geometrical form of its outline; silhouettes of the domes are similar when the vertices are superposed, irrespective of the position of the dome base which is variable. Of course, the steadiness concerns the average shape in different developmental stages, there is some variation in the silhouettes but no obvious trend in shape changing.

In barley the dome remains principally steady in shape not only during the vegetative phase, as indicated in previous paper (Hejnowicz and Włoch 1980a) but also during the generative phase the early part of which has been studied in this paper. During the vegetative phase the minimal and maximal dome height attained each plastochron increased until plastochron 13-14 (beginning of double ridge stage). The dome height is then 170-200 μm high which corresponds to 0.45 mm of the apex length measured from the vertex to the axil of the uppermost recognizable leaf by Nicholls and May (1963). In barley there is a cyclic plastochronic change of dome height superposed on developmental increase of the height, both within steady silhouette of the dome. In maize and *Agropyron*, beside this change, there is also a change in the scale of the dome: in maize the scale is slowly increasing, in *Agropyron* it attains a maximum at 12th plastochron. It follows thus that the dome growth in barley is simpler than in maize and *Agropyron*. Wheat apices appear similar to barley. SEM micrographs of *Triticum aestivum* (Gardner et al. 1985) indicate steady dome shape not only for apices of main axis from vegetative to terminal spikelet formation but also for the spikelet apices. Our hypothesis is that in general the growth of the shoot apical dome is based on a steady pattern of principal directions of growth however this basic steadiness is not always reflected in steady outline of external surface of the dome (Hejnowicz and Hejnowicz 1988).

Hejnowicz and Włoch (1980b) estimated that the relative growth rate in volume of the distal part of barley dome in vegetative phase was 5 to 10 times slower than that at the level of leaf initiation. A decrease in the rate within the uppermost frusta defined as undifferentiated stem segment without leaf primordia was also reported. The more detailed analysis of growth distribution in the present paper supports such distribution of growth. The maximum $RERG_{vol}$ occurs in the subapical zone which however in a high dome does not reach the level of leaf initiation. The lowering of the rate in the distal part is not as pronounced as it seemed to be on the basis of the distribution of mitoses in our previous paper (Hejnowicz and Włoch 1980b). Yet, the initial cell of the second tunica layer which perpetuates the germ line is within the slow growing apical zone. The zone of maximum $RERG_{vol}$ in high domes during the

transition and beginning of generative phases is separated from the dome base by a zone where the rate is low. Thus the zone of slower growth, which in younger and shorter apices was on the level of the first frustum, appears to maintain its distance from the vertex in higher domes. Though it changes the relative position in the apex since it was located above the uppermost frustum in higher dome.

It was our expectation that during the transition phase there would be an activation of the distal part of the dome as typically happens in shoot apices during this phase (Lyndon 1977). However, in fact there is not much to be activated in the distal part of barley dome. The low volumetric rate of growth ($RERG_{vol}$) in the distal part is due both to lack of anticlinal growth ($RERG_{l\,(ant)}$) within tunica and low periclinal growth ($RERG_{l\,(per)}$). Since the tunica is preserved in generative phase only this part of the $RERG_{vol}$ minimum which follows from low $RERG_{l\,(per)}$ in this part could be removed. Whether such subtle change occurs during the transition to generative phase can not be resolved.

If indeed there is steady pattern of growth rates with maximum rate at some distance, d, from the vertex the increase in height, h, of the dome in successive plastochrons must result in lowering of the mean rate of growth in volume for the whole dome per plastochron. Such trend was observed already in previous studies (Hejnowicz and Włoch 1980b) and is obvious in phases studied in this paper. We calculated the mean rate of relative rate of growth in volume for the whole dome of different height on the basis of the $RERG_{vol}$ pattern determined in this paper. The results are shown in Table 1. The calculated rates for the first four heights which correspond to the dome during plastochrons 6-9 may be compared with the data from the previous paper (1.016, 0.773, 0.740, 0.628 – Hejnowicz and Włoch 1980b) (Table 1). The values from both papers fit quite well. Although there is a decrease of the mean plastochron rate of the growth in volume for the whole dome in successive plastochrons, the mean rate may not be decreasing when calculated on the basis of calendar time unit, because successive plastochrons decrease.

Table 1

Mean relative elemental rate of growth in volume per plastochron for the whole dome evaluated on the basis of $RERG_{vol}$ map from Fig. 16

Apical dome age (in plastochrons)	6	7	8	9
Height of the dome (μm)	77	84	93	104
$RERG_{vol}$ (% plast.$^{-1}$)	0.993	0.947	0.865	0.783

The low rate of growth of the newly formed frustum during its early plastochrons compared to the rate in the dome has been observed in *Agropyron* (Smith and Rogan 1975) and can be inferred for other cereals on

the basis of similar lengths of successive uppermost frusta. This is especially apparent on young spikes during the single ridge and double ridge stages, where the successive shoot units can be easily seen (Gardner et al. 1985).

The low rate of growth of young frusta is paralleled by active growth of lateral appendages (leaf primordia, spikelets) associated with frustum. It is reasonable, as Smith and Rogan (1975) wrote, to interpret the young frustum as a weak sink for available supply of assimilates and the apical dome and leaf or spikelet primordium as strong sinks. Within a high apex the sink is stronger at some distance above the axil of youngest appendage.

This paper illustrates an application of a curvilinear coordinate system and growth tensor to real shoot apical domes. Parallel application has been done by Nakielski (1987b) for *Picea abies*. The curvilinear coordinate system and growth tensor allow the most complete three-dimensional description of growth rates in apical domes, which when combined with data on cell dimmension enable calculations of cell division rates. The latter will be presented in next paper of this series.

REFERENCES

Abbe E. C., Phinney B. O., 1951. The growth of the shoot apex in maize: external features. Amer. J. Bot. 38: 734-744.

Gardner J. S., Hess W. M., Trione E. J., 1985. Development of the young wheat spike: A SEM study of Chinese spring wheat. Amer. J. Bot. 72: 548-559.

Hejnowicz Z., 1984. Trajectories of principal directions of growth, natural coordinate system in growing plant organ. Acta Soc. Bot. Pol. 53: 29-42.

Hejnowicz Z., Hejnowicz K., 1988. Computer modeling of growth in root apices. Planta (in press).

Hejnowicz Z., Nakielski J., Hejnowicz K., 1984a. Modeling of spatial variations of growth within apical domes by means of the growth tensor. I. Growth specified on dome axis. Acta Soc. Bot. Pol. 53: 17-28.

Hejnowicz Z., Nakielski J., Hejnowicz K., 1984b. Modeling of spatial variations of growth within apical domes by means of the growth tensor. II. Growth specified on dome surface. Acta Soc. Bot. Pol. 53: 301-316.

Hejnowicz Z., Romberger J. A., 1984. Growth tensor of plant organs. J. Theor. Biol. 110: 93-114.

Hejnowicz Z., Włoch W., 1980a. Growth and development of shoot apex in barley. I. Morphology and histology of shoot apex in vegetative phase. Acta Soc. Bot. Pol. 49: 21-31.

Hejnowicz Z., Włoch W., 1980b. Growth and development of shoot apex in barley. II. Distribution of growth rates during vegetative phase. Acta Soc. Bot. Pol. 49: 33-48.

Lyndon R. F., 1977. Interacting processes in vegetative development and in the transition to flowering at the shoot apex. In: Integration of activity in the higher plants. Symp. Soc. Exp. Biol. 31: 221-250.

Nakielski J., 1987a. Spatial variations of growth within domes having different patterns of principal growth directions. Acta Soc. Bot. Pol. 56: 611-623.

Nakielski J., 1987b. Variations of growth in shoot apical domes of spruce seedlings: A study using the growth tensor. Acta Soc. Bot. Pol. 56: 625-643.

Nicholls P. B., May L. H., 1963. Studies on the growth of the barley apex. Aust. J. Biol. Sci. 16: 561-571.

Rogan P. G., Smith D. L., 1974. The development of the shoot apex of *Agropyron repens* (L.). Beauv. Ann. Bot. 38: 967-976.
Smith D. L., Rogan P. G., 1975. Growth of the stem of *Agropyron repens* (L.). Beauv. Ann. Bot. 39: 871-880.

Wzrost i rozwój wierzchołka pędu jęczmienia. III. Badanie zmienności szybkości wzrostu za pomocą tensora wzrostu

Streszczenie

Pokazano jak stosować metodę tensora wzrostu i naturalny układ współrzędnych do opisu rozmieszczenia szybkości wzrostu wewnątrz konkretnego organu, w tym przypadku wierzchołka pędu jęczmienia w okresie przejścia z fazy wegetatywnej w generatywną. Apikalna część wierzchołka u jęczmienia ma niezmieniający się podczas wzrostu kształt, który można opisać elipsą w przekroju osiowym. Wysokość części apikalnej powiększa się z wiekiem wierzchołka. W części apikalnej realizowana jest elongacja; szybkość elongacji zmniejsza się w miarę wzrostu wysokości. Układ kompleksów komórek w protodermie wskazuje na to, że wzrost powierzchniowy na powierzchni wierzchołka jest anizotropowy — kompleksy wydłużają się w kierunku meridionalnym ze wzrostem odległości od szczytu. Długość pakietów komórek w funkcji odległości od szczytu zmienia się mniej więcej jednakowo w wierzchołkach w różnym wieku.

Modelowanie matematyczne realizowano w naturalnym układzie współrzędnych, który powstał ze zlepienia w części bazalnej dwóch układów krzywoliniowych: wydłużonego sferycznego i cylindrycznego. Prędkość przesunięć elementów i pochodną tej prędkości wzdłuż linii meridionalnej otrzymano metodą graficzną na podstawie analizy sekwencji pakietów komórek. Okazało się, że taka analiza pozwala odtworzyć rzeczywistą zależność między pozycją elementu na powierzchni a czasem. Uzyskano następujące rozmieszczenie szybkości wzrostu objętościowego we wnętrzu wierzchołka: maksimum $RERG_{vol}$ jest w strefie subdystalnej, nieco mniejsze szybkości są w strefie dystalnej i peryferycznej, najmniejsze przy podstawie. Średnia szybkość wzrostu objętościowego, liczona na całą objętość apikalnej części wierzchołka, zmniejsza się w miarę jak powiększa się wysokość tej części, tzn. z wiekiem wierzchołka.